

High-resolution Spatio-temporal Model for County-level COVID-19 Activity in the U.S.

Shixiang Zhu¹, Alexander Bukharin¹, Liyan Xie¹, Mauricio Santillana², Shihao Yang¹, and Yao Xie¹

¹School of Industrial and Systems Engineering, Georgia Institute of Technology

²Harvard Medical School, Computational Health Informatics Program, Harvard University
School of Engineering & Applied Sciences

Abstract

We present an interpretable high-resolution spatio-temporal model to estimate COVID-19 deaths together with confirmed cases one-week ahead of the current time, at the county-level and weekly aggregated, in the United States. A notable feature of our spatio-temporal model is that it considers the (a) temporal auto- and pairwise correlation of the two local time series (confirmed cases and death of the COVID-19), (b) dynamics between locations (propagation between counties), and (c) covariates such as local within-community mobility and social demographic factors. The within-community mobility and demographic factors, such as total population and the proportion of the elderly, are included as important predictors since they are hypothesized to be important in determining the dynamics of COVID-19. To reduce the model’s high-dimensionality, we impose sparsity structures as constraints and emphasize the impact of the top ten metropolitan areas in the nation, which we refer (and treat within our models) as *hubs* in spreading the disease. Our retrospective out-of-sample county-level predictions were able to forecast the subsequently observed COVID-19 activity accurately. The proposed multi-variate predictive models were designed to be highly interpretable, with clear identification and quantification of the most important factors that determine the dynamics of COVID-19. Ongoing work involves incorporating more covariates, such as education and income, to improve prediction accuracy and model interpretability.

1 Introduction

The global spread of COVID-19, the disease caused by the novel coronavirus SARS-CoV-2, has affected nearly everyone’s lives on the planet. Even the largest economies’ resources have been strained due to the large infectivity and transmissibility of COVID-19. As the number of cases of COVID-19 continues increasing, understanding finer-grained spatio-temporal dynamics of this disease as well as some of the leading factors affecting disease transmissions, such as community mobility and population, is critical to helping officials make policy decisions and curb the further spread of the disease.

Most of the previous research aimed at studying the spread of COVID-19 has focused on two key measurements: the number of confirmed cases and the number of deaths. Cases going up or down over time shed light on the rate of spread of COVID-19 at a given point in time — but it is only valid if enough people get tested. The limited testing ability resulted in a serious underestimation of COVID-19 cases in the pandemic’s early stages [20]. For example, when there was not enough testing capacity, as was the case in New York City in March 2020, the number of cases reported was clearly an undercount of true cases, estimated to be much larger (up by a factor of 10) [14, 24]. Some studies have circumvented the problem of underestimation by considering the case positivity rate, which measures the percentage of total COVID-19 tests conducted that are positive. However, most of the widely-used COVID-19 data sets, such as the *COVID Tracking Project* [29], only collect the total number of people with a completed polymerase chain reaction (PCR) test that returns positive as reported by the state or territory, which has a much lower spatial resolution (state-level) in comparison with the cases and deaths data (county-level). Such coarse-grained

testing numbers would introduce extra noise to our model and would most likely be incapable of improving the confirmed cases prediction accuracy at the county level. Deaths are also an important metric that most people care about when it comes to the virus’s ultimate epidemiological impact. In contrast to the number of confirmed cases, the number of deaths is a good and accurate indicator for evaluating how serious a burden this pandemic is causing, not only on health care systems but also on the general public’s mental health and well-being. Some epidemiological studies, such as [19], also recommend tracking deaths, even though deaths lag behind new cases, typically by two weeks to a month.

A large amount of fine-grained data offers a unique opportunity to study the disease’s spread dynamics from a micro-level view. For the United States, a number of teams have been working on collecting comprehensive COVID-19 tracking data, including counts of cases and deaths at the county-level on a daily basis. Such kind of data gives us a general picture of how the virus is spreading across metropolitan and micropolitan counties and how such dynamics are evolving over time. Aside from considering the cases and the deaths, we also aim to study other important local factors in the transmission of the COVID-19. Recent studies [23] on the spread of COVID-19 show that besides the distance to the epicenter, other factors, such as subway and airport, are positively connected with the virus transmission. Moreover, both urban areas and population density are positively associated with the spread of COVID-19 after the outbreak. The proportion of the elderly population has also been identified as a key factor in the death rate. Therefore, we consider the within-community mobility and two critical demographic factors by taking advantage of the COVID-19 Community Mobility Reports [12] and the American Community Survey (ACS) [3]. These two data sets are publicly available and include detailed county-level statistics that provide insights into what has changed in response to policies aimed at combating the COVID-19 and what factors may affect the disease’s transmission. As illustrated in Fig. 1, in our model, we assume the numbers of cases and deaths in each county to depend on the neighboring counties and major metropolitan areas in the U.S., which we refer as *hubs* in spreading the disease. Local community mobility and demographic factors, including population and elderly population, are considered local covariates in the model, which also play a crucial role in the final number of deaths.

In this paper, we use a data-driven method incorporating a large-scale data set from multiple sources to predict the deaths and the confirmed cases of COVID-19 at the county level in the United States. To improve our model’s reliability and performance, we emphasize recovering county-level deaths’ trajectories

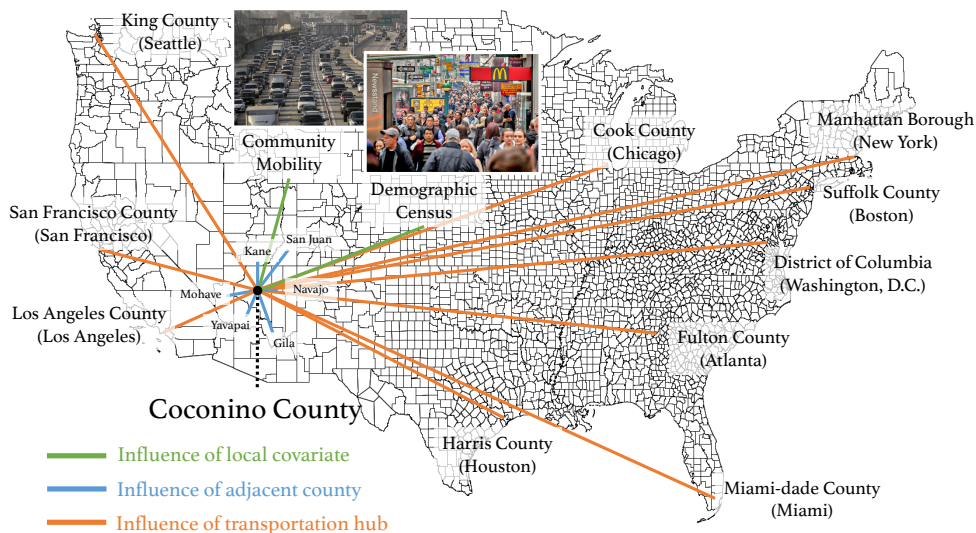


Figure 1: An example of spatio-temporal covariates in our model for Coconino County, Arizona. Based on the counties in the U.S. as fundamental units, we assume the number of confirmed cases and deaths of COVID-19 reported in a given county are jointly related to the numbers reported in its adjacent counties (they are Kane, San Juan, Navajo, Gila, Yavapai, Mohave for Coconino in this example) and ten selected nationwide hubs (including San Francisco, Los Angeles, Seattle, Chicago, Atlanta, Miami, Washington, D.C., Boston, and New York). These two numbers also depend on some local covariates, such as community mobility level and some county’s demographic factors.

and focus less on improving confirmed cases’ predictive accuracy. Our method’s most notable contribution is considering the spatial structure among hubs and neighboring counties in modeling the cross-correlation between cases and deaths. We also present the effect of a wide variety of geographic community mobility and social demographic factors on the spread of COVID-19. Our approach drastically differs from previous studies [7, 2, 1], in which the number of cases and deaths, and other covariates, including the community mobility and social demographic factors, are inter-linked through a vector autoregressive process. Our model shows that these hubs play a pivotal role in spreading the disease. We also find that both cases and deaths are significantly related to the total population at the local level and that deaths are also positively associated with the proportion of the elderly population. Additionally, we found that confirmed cases are not significantly related to the proportion of the elderly population, which may prove that the disease was mostly circulating among young people in its later stage. In particular, while we identify a spike in cases since the beginning of the summer, we do not observe a clear spike in deaths. This may be explained by the fact that a larger proportion of young people, who are generally at lower risk of death, were infected in the more recent pandemic stages.

The remainder of the article is organized as follows. We first review related works in the rest of this section, followed by describing the data sets we have used in Section 2. Section 3 presents our proposed vector autoregressive model with spatial structure incorporated. We demonstrate the effectiveness of our model and discuss its interpretation in Section 4. Lastly, the article concludes with discussions and future research directions in Section 5.

Related work Compartmental models have been widely used in infectious disease epidemiological studies. In the SIR model [13], one of the simplest compartmental models, the population is assigned to three components: S (susceptible), I (infectious), and R (recovered). These variables (S, I, and R) represent the number of people in each compartment. The transition between different compartments is modeled using a set of coupled differential equations. Based on the SIR model, many variants have been proposed in the last decades, including the SIRD model [10, 4] that considers deceased individuals, and the SEIR model [15, 33, 16] that considers exposed period during which individuals have been infected but are not yet infectious themselves, to name a few. The total population is usually assumed to be fixed in the compartmental models; therefore, it works well when modeling nationwide data. However, in our high-resolution modeling, each county’s population is of high variability due to dynamics across the county. Therefore, we use a spatio-temporal model instead to capture the influence of major big cities and neighboring counties without fixing each county’s population.

Studies evaluating the spatial spread of the COVID-19 pandemic are scarce [27]. However, understanding the spatial spread of the COVID-19 outbreak is critical to predicting local outbreaks and developing public health policies during the early stages of COVID-19. Previous studies have described the spatial spread of severe acute respiratory syndrome (SARS) in Beijing and mainland China [25, 9, 18, 17, 8] using limited or localized data. One study also considered the different types of connections between a few cities to calculate the spatial association [25]. There is also prior work using the multivariate Hawkes process to model the conditional intensity of new COVID-19 cases and deaths in the U.S. at the county level [5], without considering the influence of the big cities and other important demographic factors.

There are also various efforts studying impacts from other aspects, such as temperature, humidity [30, 28], age, gender [8], and travel restrictions [6, 21]. Most of these studies are constrained on a relatively small scale because of limited data at the early stage of the pandemic.

2 Data

We have used three comprehensive datasets in this study, including confirmed cases and deaths of COVID-19, community mobility data, and demographic census data. These datasets play an important role in helping us understand the spatio-temporal dynamics of COVID-19 transmission.

Confirmed cases and deaths of COVID-19 We used the dataset from The New York Times [32], which are based on reports from state and local health agencies. The data is the product of dozens of journalists working across several time zones to monitor news conferences, analyze data releases, and seek

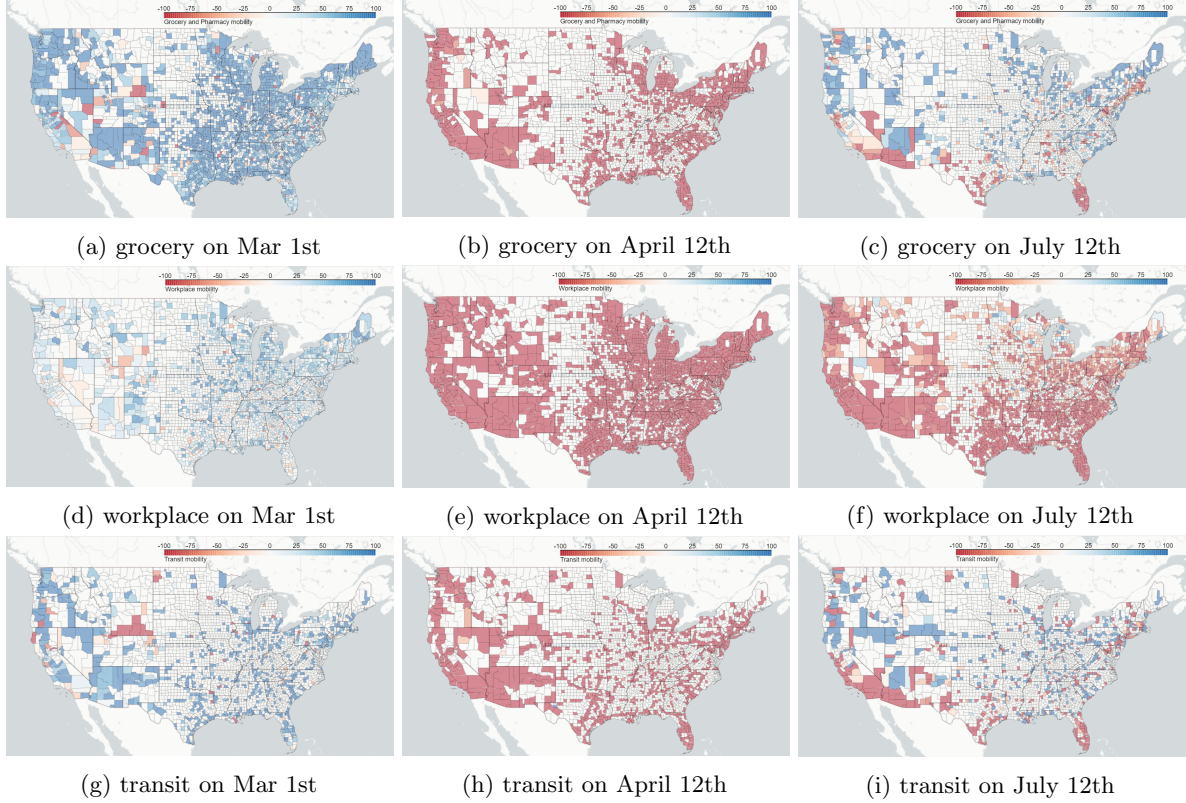


Figure 2: Overview of Google mobility data in three selected categories: grocery, workplace, and transit on three different days. Counties in red and blue indicate their mobility is lower and higher than the normal level, respectively. The mobility level varies over time and space due to local government policy change in response to COVID-19.

public officials’ clarification on how they categorize cases. The data includes two parts: (i) *confirmed cases* are counts of individuals whose coronavirus infections were confirmed by a laboratory test and reported by a federal, state, territorial, or local government agency. Only tests that detect viral RNA in a sample are considered confirmatory. These are often called molecular or reverse transcription-polymerase chain reaction (RT-PCR) tests; (ii) *confirmed deaths* are individuals who have died and meet the definition for a confirmed COVID-19 case. Some states reconcile these records with death certificates to remove deaths from their count, where COVID-19 is not listed as the cause of death. This data have removed non-COVID-19 deaths among confirmed cases according to the information released by health departments, i.e., in homicide, suicide, car crashes, or drug overdose. All cases and deaths are counted on the date they are first announced. In practice, we have observed periodic weekly oscillations in daily reported cases and deaths, which could have been caused by testing bias (higher testing rates on certain days of the week). To reduce such bias, we aggregate the number of cases and deaths of each county *by week*.

Community mobility As global communities respond to COVID-19, we’ve heard from public health officials that the same type of aggregated, anonymized insights we use in products such as Google Maps could be helpful as they make critical decisions to combat COVID-19. The COVID-19 Community Mobility Reports [12] aim to provide insights into what has changed in response to policies aimed at combating COVID-19. The reports record people’s movement by county daily, across different categories such as retail and recreation, groceries and pharmacies, parks, transit stations, workplaces, and residential. The data shows how visitors to (or time spent in) categorized places change compared to the baseline days (in percentage). The negative percentage represents the level of mobility is lower than the baseline, and the positive percentage represents the opposite. A baseline day represents a normal value for that day of the week. The baseline day is the median value from the five-week period from January 3rd to February 6th, 2020. To match the temporal

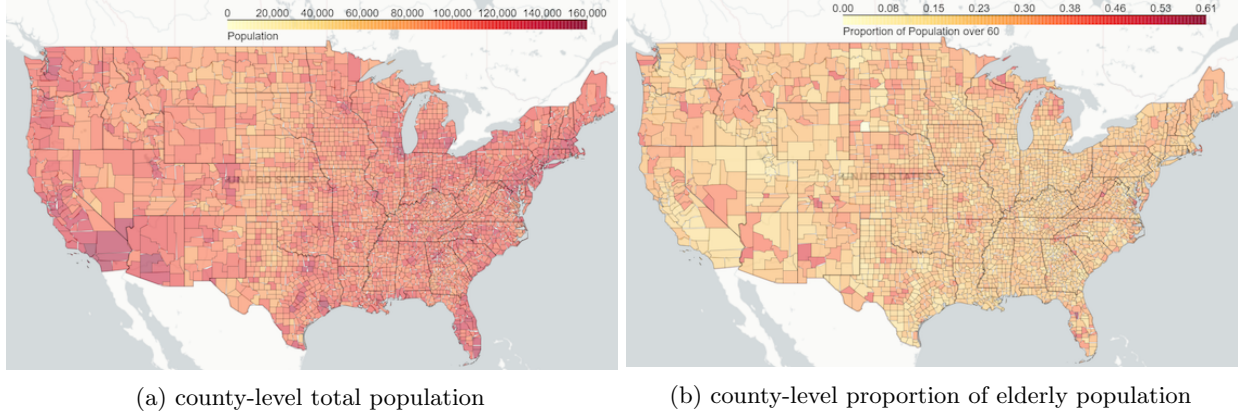


Figure 3: Overview of the social demographic factors. The color depth represents the value of the demographic variables of interest in certain county.

resolution with the COVID-19 data and detrend the weekly pattern, we aggregate each county’s mobility data by week. Examples of three categories have been shown in Fig. 2.

Demographic census Data from the American Community Survey (ACS) [3], provided by the U.S. Census Bureau, is the comprehensive source for comprehensive information about the population, demographic, and economic status of each zip code region in the U.S. Unlike the census data, which takes place every ten years, the ACS is conducted every year. The latest ACS data are available in the year 2018. Some demographic factors are particularly useful for us in understanding how population distribution affects the spread of disease (by correlating the local socio-economic profile with its confirmed cases and deaths), and these factors contain essential information about the development and economic growth of different areas. To match the spatial resolution with the COVID-19 data, we aggregate the zipcode regions’ demographic data in the same county. We selected two leading factors that affect the spread and the infection of the disease, i.e., total population, and the proportion of the elderly with an age of 65 or older [26].

3 Methodology

This section presents our statistical model that captures the spatio-temporal dynamics of the spread of COVID-19. We begin with a brief description of the problem setup and notations, then jointly model confirmed cases and deaths as a vector autoregressive process in Section 3.2. The essential notations defined in this section are also summarized in Table 1.

3.1 Problem setup and notations

Consider confirmed cases and deaths of the COVID-19 in N counties and T weeks (recall that we aggregated these numbers by week to reduce bias). Let $\mathcal{I} = \{i = 1, \dots, N\}$ be the set of counties and $\mathcal{T} = \{t = 1, \dots, T\}$ be the set of weeks starting from February 9th until August 9th. We assume there is a set of counties $\mathcal{I}' = \{i = 1, \dots, N'\} \subset \mathcal{I}$ playing a significant role in spreading the disease due to their high population density and well-developed transportation network connecting to other major cities in the U.S.. We refer to these counties as *hubs*, and the selected hubs are marked in Fig. 1. Denote the number of confirmed cases and deaths in county $i \in \mathcal{I}$ and week $t \in \mathcal{T}$ as $c_{i,t} \in \mathbb{Z}_+$ and $d_{i,t} \in \mathbb{Z}_+$, respectively. In our setting, $T = 27$, $N = 3144$, and $N' = 10$.

We also consider K mobility categories and L demographic factors as covariates of the model, where $K = 6$ and $L = 2$. Let $\mathcal{K} = \{k = 1, \dots, K\}$ be the set of community mobility categories and $\mathcal{L} = \{l = 1, \dots, L\}$ be the set of demographic factors. Denote the mobility score in category $k \in \mathcal{K}$ for county $i \in \mathcal{I}$ in week $t \in \mathcal{T}$ as $m_{i,k,t} \in \mathbb{R}$, and denote the data of demographic factor $l \in \mathcal{L}$ for county $i \in \mathcal{I}$ as $z_{i,l} \in \mathbb{R}_+$. Let $\mathbf{c}_t := [c_{1,t}, \dots, c_{N,t}]^\top$ and $\mathbf{d}_t := [d_{1,t}, \dots, d_{N,t}]^\top$ denote the confirmed cases and deaths in week $t \in \mathcal{T}$,

Table 1: Summary of essential notations

Section	Notation	Description
3.1	$\mathcal{T} = \{t = 1, \dots, T\}$	Set of all weeks.
	$\mathcal{I} = \{i = 1, \dots, N\}$	Set of all counties.
	$\mathcal{K} = \{k = 1, \dots, K\}$	Set of mobility categories.
	$\mathcal{L} = \{l = 1, \dots, L\}$	Set of demographic factors.
	$c_{i,t} \in \mathbb{Z}_+$	Number of confirmed cases for county $i \in \mathcal{I}$ in week $t \in \mathcal{T}$.
	$d_{i,t} \in \mathbb{Z}_+$	Number of deaths for county $i \in \mathcal{I}$ in week $t \in \mathcal{T}$.
	$z_{i,l} \in \mathbb{R}_+$	Data of demographic factor $l \in \mathcal{L}$ for county $i \in \mathcal{I}$.
3.2	$m_{i,k,t} \in \mathbb{R}$	Data of mobility category $k \in \mathcal{K}$ for county $i \in \mathcal{I}$ in week $t \in \mathcal{T}$.
	$\mathcal{A} = \{(i, j) : i, j \in \mathcal{I}\}$	Set of all county pairs in the U.S. that i, j are adjacent to each other or one of i, j is a <i>hub</i> .
	$\mathbf{B}_\tau = (\beta_{i,j}) \in \mathbb{R}^{N \times N}$	Coefficients of past confirmed cases between county $i, j \in \mathcal{I}$ for τ weeks ago.
	$\mathbf{A}_\tau = (\alpha_{i,j}) \in \mathbb{R}^{N \times N}$	Coefficients of past deaths between county $i, j \in \mathcal{I}$ for τ weeks ago.
	$\mathbf{H}_\tau = (h_{i,j}) \in \mathbb{R}^{N \times N}$	Coefficients of past confirmed cases between county $i, j \in \mathcal{I}$ for τ weeks ago.
	$\mu_{k,\tau} \in \mathbb{R}$	Coefficient for mobility category $k \in \mathcal{K}$ in the past τ -th week w.r.t. the number of cases.
	$\nu_{k,\tau} \in \mathbb{R}$	Coefficient for mobility category $k \in \mathcal{K}$ in the past τ -th week w.r.t. the number of deaths.
	$v_l \in \mathbb{R}$	Coefficient for demographic factor $l \in \mathcal{L}$ w.r.t. the number of cases.
	$\zeta_l \in \mathbb{R}$	Coefficient for demographic factor $l \in \mathcal{L}$ w.r.t. the number of deaths.

respectively. Let $\mathbf{m}_{k,t} := [m_{1,k,t}, \dots, m_{N,k,t}]^\top$ denote the score of community mobility category $k \in \mathcal{K}$ for all counties $i \in \mathcal{I}$ in week $t \in \mathcal{T}$. Let $\mathbf{z}_l := [z_{1,l}, \dots, z_{N,l}]^\top$ denote the data of demographic factor $l \in \mathcal{L}$ for all counties $i \in \mathcal{I}$.

3.2 Spatio-temporal model

We consider a linear spatio-temporal autoregressive model where the number of confirmed cases (\mathbf{c}_t) and deaths (\mathbf{d}_t) is a time series regressed on their previous values and the mobility covariate $\mathbf{m}_{k,t}$ and demographic covariate \mathbf{z}_l . Denote the time window's length that we consider in the past (the memory depth) as p . Based on previous studies [31], it is known that the COVID-19 virus has an incubation period of around two weeks. Therefore, we choose $p = 2$ throughout this paper.

Define the augmented observation vector as (which contains both confirmed case and death counts):

$$\mathbf{x}_t := \begin{bmatrix} \mathbf{c}_t \\ \mathbf{d}_t \end{bmatrix} \in \mathbb{R}^{2N}.$$

Then our spatio-temporal model can be written as a vector autoregressive (VAR) process:

$$\mathbf{x}_t = \sum_{\tau=1}^p \mathbf{\Lambda}_\tau \mathbf{x}_{t-\tau} + \sum_{k=1}^K \sum_{\tau=1}^p \gamma_{k,\tau} \otimes \mathbf{m}_{k,t-\tau} + \sum_{l=1}^L \omega_l \otimes \mathbf{z}_l + \boldsymbol{\epsilon}_t, \quad \boldsymbol{\epsilon}_t \sim \mathcal{N}\left(\mathbf{0}, \begin{bmatrix} \boldsymbol{\Sigma}_\eta & \mathbf{0} \\ \mathbf{0} & \boldsymbol{\Sigma}_\eta \end{bmatrix}\right), \quad (1)$$

where \otimes is the Kronecker product and

$$\mathbf{\Lambda}_\tau = \begin{bmatrix} \mathbf{B}_\tau & \mathbf{0} \\ \mathbf{H}_\tau & \mathbf{A}_\tau \end{bmatrix} \in \mathbb{R}^{2N \times 2N}, \quad \gamma_{k,\tau} = \begin{bmatrix} \mu_{k,\tau} \\ \nu_{k,\tau} \end{bmatrix} \in \mathbb{R}^2, \quad \omega_l = \begin{bmatrix} v_l \\ \zeta_l \end{bmatrix} \in \mathbb{R}^2, \quad \boldsymbol{\epsilon}_t = \begin{bmatrix} \boldsymbol{\epsilon}_{t,c} \\ \boldsymbol{\epsilon}_{t,d} \end{bmatrix} \in \mathbb{R}^{2N}, \quad 1 \leq \tau \leq p.$$

In our model (1), the first-term captures the dependence on past confirmed cases and deaths; the second term captures the influence of past local community mobility; the third term captures the influence of local demography, which is held constant over time. Specifically, \mathbf{B}_τ and \mathbf{A}_τ contain the autoregressive coefficients for the number of confirmed cases and deaths, respectively; \mathbf{H}_τ describes the dependence of the current number of deaths on the number of confirmed cases in τ weeks ago. These three matrices share the same sparse spatial structure, where entry at (i, j) is zero if county i and county j is not adjacent, and none of them is the hub. Formally, the set of adjacency pairs is defined by $\mathcal{A} = \{(i, j) \in \mathcal{I} : (i, j) \text{ is an edge of the graph } \mathcal{G}\}$; each node of \mathcal{G} denotes a county, and there is an edge between two nodes whenever the corresponding counties are geographically adjacent or one of them is a hub. The $\mu_{k,\tau}$, $\nu_{k,\tau}$, v_l , and ζ_l are four scalar coefficients. To be specific, $\mu_{k,\tau}$, $\nu_{k,\tau}$ represent the coefficients for the local community mobility score in category k in τ weeks ago with respect to the corresponding number of confirmed cases and deaths, respectively. Similarly,

v_l, ζ_l represent the coefficients for local demographic factor l with respect to the corresponding number of confirmed cases and deaths, respectively. The spatial covariance matrix between the noise at counties i and j is denoted as the (i, j) -th entry of Σ_η ; it is a function of their Euclidean distance s_{ij} and is parameterized by η . Some commonly used spatial models include: Gaussian model [22], Exponential model [11], and Matérn model [11]. Here we adopt the exponential spatial covariance model $\Sigma_\eta(i, j) = \eta \exp\{-\eta s_{ij}\}$, where η is a pre-specified parameter, which controls the rate of spatial decay. In this paper, we specify a reasonable value of the parameter $\eta = 10^3$.

We aim to fit the model (1) for confirmed cases and deaths jointly by minimizing the *prediction error*. Define the set of parameters $\theta = \{\Lambda, \omega, \gamma\} \in \Theta$, where Θ is the set containing all feasible values. For a pre-specified hyper-parameter $\delta \in [0, 1]$, the loss function is defined as a weighted combination of quadratic loss functions for death and confirmed case residuals:

$$\ell(\theta) := \delta \sum_{t=1}^T \varepsilon_{t,d}^\top \Sigma_\eta^{-1} \varepsilon_{t,d} + (1 - \delta) \sum_{t=1}^T \varepsilon_{t,c}^\top \Sigma_\eta^{-1} \varepsilon_{t,c}, \quad (2)$$

where $\varepsilon_{t,c}$ denotes the confirmed case prediction residual

$$\varepsilon_{t,c} = [\mathbf{I} \quad \mathbf{0}] \left(\mathbf{x}_t - \sum_{\tau=1}^p \Lambda_\tau \mathbf{x}_{t-\tau} - \sum_{k=1}^K \sum_{\tau=1}^p \gamma_{k,\tau} \otimes \mathbf{m}_{k,t-\tau} - \sum_{l=1}^L \omega_l \otimes \mathbf{z}_l \right),$$

and $\varepsilon_{t,d}$ denotes the death prediction residual

$$\varepsilon_{t,d} = [\mathbf{0} \quad \mathbf{I}] \left(\mathbf{x}_t - \sum_{\tau=1}^p \Lambda_\tau \mathbf{x}_{t-\tau} - \sum_{k=1}^K \sum_{\tau=1}^p \gamma_{k,\tau} \otimes \mathbf{m}_{k,t-\tau} - \sum_{l=1}^L \omega_l \otimes \mathbf{z}_l \right).$$

The hyper-parameter δ controls the proportion of death prediction loss. In practical terms, we emphasize the importance of death, and hence we choose $\delta = 0.9$ empirically. The reason is that it is known that the confirmed cases are quite noisy and can depend on the capacity of testings.

The parameters θ can be estimated by solving the following optimization with a regularization function:

$$\min_{\theta \in \Theta} \ell(\theta) + \lambda_1 R(\theta), \quad (3)$$

where $\lambda_1 \geq 0$ is a parameter that controls the importance of the regularization term, and $R(\theta)$ is the elastic net type regularization function (with hyper-parameter $\lambda_2 \in [0, 1]$) given by

$$R(\theta) := \sum_{\tau=1}^p \sum_{i=1}^N \sum_{j=1}^N \mathbb{1}_A\{(i, j)\} \left[\lambda_2 \left(|\alpha_{i,j,\tau}| + |\beta_{i,j,\tau}| + |h_{i,j,\tau}| \right) + (1 - \lambda_2) \left(|\alpha_{i,j,\tau}|^2 + |\beta_{i,j,\tau}|^2 + |h_{i,j,\tau}|^2 \right) \right],$$

where $\mathbb{1}_A\{x\}$ is the indicator function, i.e., taking the value 1 if $x \in A$ otherwise 0; λ_2 is the ℓ_1 penalty ratio in the regularization function; $\alpha_{i,j,\tau}, \beta_{i,j,\tau}, h_{i,j,\tau}$ are the entries of matrices $\mathbf{A}_\tau, \mathbf{B}_\tau, \mathbf{H}_\tau$, respectively.

3.3 Exploit sparsity and structure to solve large-scale optimization problems

Our model's salient feature is that we consider the underlying spatio-temporal structure between the number of confirmed cases and deaths. If there is no specific structure in coefficient matrices, our methods looks on the surface to be a naive linear model but requires to solve a large-scale high-dimensional optimization problem, which contains 79,077,916 parameters (variables in the optimization problem) with only 84,888 data points. Instead of solving such difficult problems directly, we tackle this challenge by exploiting the sparse spatial structure and only consider the correlation between adjacent counties and hubs, which leads to a significant reduction in the number of parameters (less than 80,000). In addition, the lower triangular structure of Λ_τ matrix (including $\mathbf{B}_\tau, \mathbf{H}_\tau$, and \mathbf{A}_τ) captures the causal relationship we believe exists in the confirm case to the death count, but not the other way around. To be exact, we assume the number of confirmed cases in the past will result in the change of both the confirmed cases and deaths in the future, while the number of deaths only relates to the future's deaths.

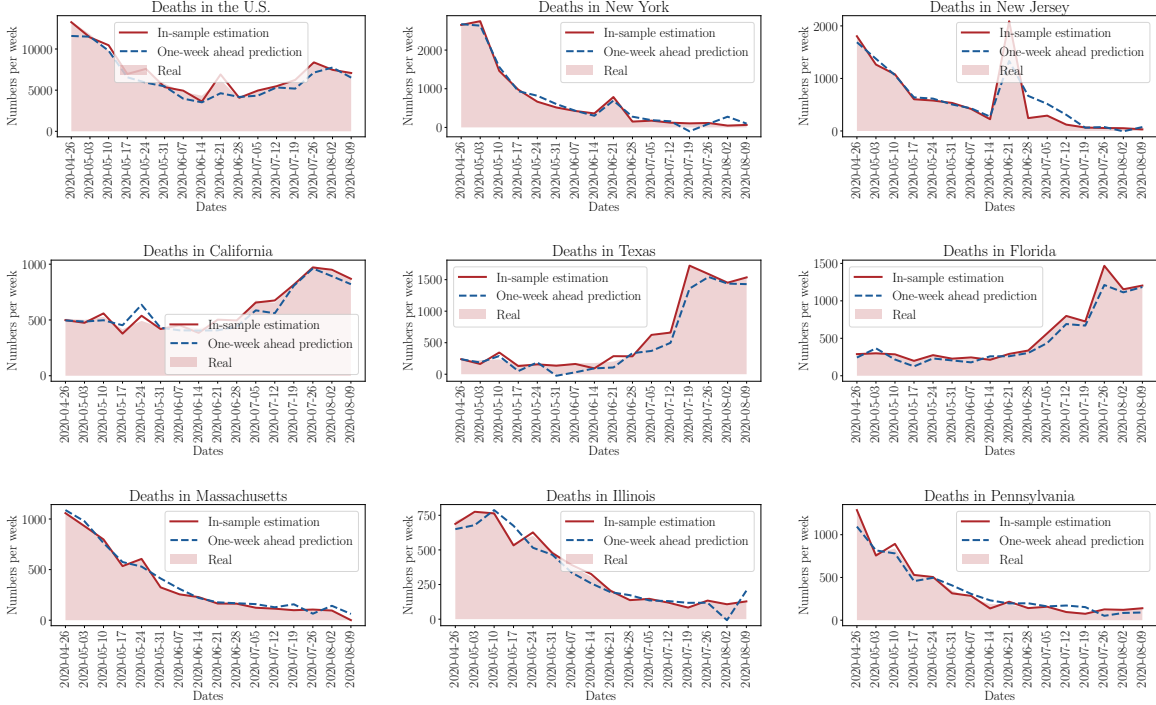


Figure 4: In-sample estimated deaths (red lines) and the one-week ahead prediction (blue dash lines) for the U.S. and other eight major states with the highest number of COVID-19 deaths in the U.S. Figures are sorted in descending order of the total number of deaths since February 9th, 2020. The results show that our model can perfectly recover the death trajectories and attain promising performance in the one-week ahead prediction.

The regularization term we devised in Section 3.2 also plays a big part in achieving the ideal results. This elastic net-based method linearly combines the lasso and ridge regression penalties on \mathbf{B}_τ , \mathbf{H}_τ , and \mathbf{A}_τ to encourage sparse spatial correlation and stabilize the solution at the same time. The hyper-parameters λ_1 and λ_2 in the regularization term are chosen by 5-fold cross-validation, where the optimal choices are $\lambda_1 \approx 10^2$ and $\lambda_2 \approx 10^{-1}$ for the fitted model.

Here we solve the optimization problem by gradient descent. To fit the model, we first standardize the data of covariates and feed all the data as a single batch in one iteration, then descend the gradients of the parameters with respect to the loss defined in (2) until the model converges. To perform a one-week ahead prediction, we feed all the data before that week as a single batch in one iteration and follow the same gradient descent procedure described above. The model normally takes about 500 iterations to reach the convergence with $\ell(\boldsymbol{\theta}) \approx 1.41 \times 10^3$.

4 Results

Now we report the results of our study. First, we describe the validation of the proposed modeling method by evaluating the in-sample estimation error. We also compare our approach against a trivial reference model, which is the persistence model. Then we demonstrate the explanatory components of our model by showing the spatio-temporal dynamics between the number of COVID-19 cases and other covariates discovered from our fitted model.

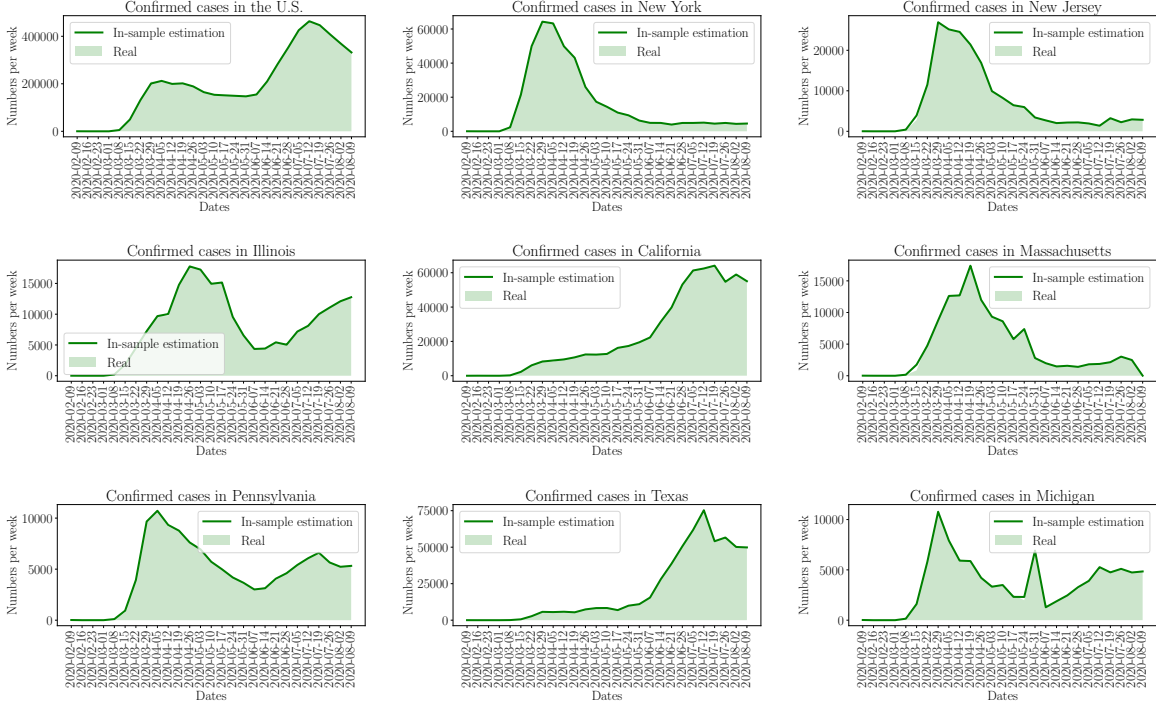


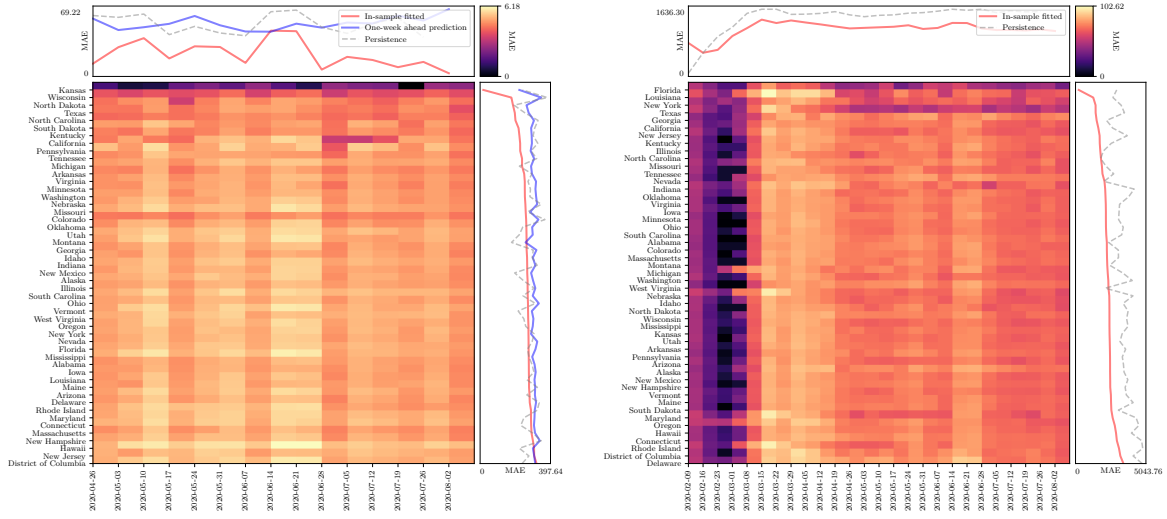
Figure 5: In-sample estimated confirmed cases (green lines) for the U.S. and other eight major states with the highest number of COVID-19 confirmed cases in the U.S. Figures are sorted in descending order of the total number of confirmed cases since February 9th, 2020. The results show that our model can perfectly recover the confirmed cases trajectories.

4.1 Model evaluation

To evaluate our method, we first compared the county-level in-sample estimation on deaths and confirmed cases using our model. The county-level in-sample estimation includes all the confirmed cases and deaths for 3,144 counties and the past 27 weeks. We fit the model using the entire data set from February 9th, 2020 to August 9th, 2020, and estimate the parameters according to (1) for each county at each week afterward. To be specific, the upper half of \mathbf{x}_t on the left-hand side of (1) is the estimated number of confirmed cases at week t , and the lower half is the estimated number of deaths at week t . For deaths count, we only present the results from April 26th, 2020, because data before May is accurate because of the low testing rate. Here, for the ease of presentation, we only focus on the mainland and do not consider Hawaii, Alaska, and other unincorporated territories of the United States in this paper.

We report the results of in-sample estimation by aggregating the county-level estimated numbers in the same state. As shown in Fig. 4, we select eight major states with the highest total number of deaths in the U.S.. The shaded area indicates the true number of deaths reported in the COVID-19 data set, and the red line indicates the in-sample estimated deaths by our model. In addition to the in-sample estimation, we also show the one-week ahead prediction in death represented by blue dash lines. The prediction at one week is obtained by fitting an individual model using the data in the past of that week and estimating the fitted model next week. We observe that the red lines perfectly match the true death trajectories and the blue dash line present promising predictive performance in the number of deaths. We also report the state-level in-sample estimated confirmed cases in Fig. 5. Similarly, the shaded area indicates the true number of confirmed cases reported in the COVID-19 data set, and the green line indicates the in-sample estimated confirmed cases by our model. The results further confirm that our model can also “recover” the confirmed cases’ trajectories with relatively high accuracy.

More quantitative results are summarized in Fig. 6. The heatmaps show the mean absolute error (MAE) of the county-level estimation within a particular state and at certain weeks. The average MAEs over states



(a) MAE for estimated death

(b) MAE for estimated confirmed case

Figure 6: Mean absolute error (MAE) of in-sample county-level estimation by our model comparing to the persistence model. These two heatmaps’ color depth indicates the MAE level of county-level prediction for certain state and week. The horizontal line chart shows the average MAE of county-level prediction over weeks. The vertical line chart shows the average MAE of county-level prediction over states. The states have been sorted in the ascending order of their MAE from top to bottom.

and weeks are presented in the vertical line chart on the right and the horizontal line chart on the top. The states are sorted in the ascending order of their MAE from top to bottom. As shown in both Fig. 6 (a) and (b), our estimation significantly outperforms the persistence model regarding the MAE. We can also observe that: for the confirmed cases, our model tends to achieve better performance for the states with larger populations, such as Florida, New York, Texas, etc.; for the deaths, our model has a balanced performance in each state, and the MAE is getting better (smaller) and becoming more stable after the summer surge of the COVID-19 (from June to July).

4.2 Model interpretation

Our study focuses on exploring the in-sample explanatory content of predetermined factors in our model. We fit the model using the entire data set collected from three data mentioned above sources in Section 2, and interpret the model by examining its fitted coefficients.

Spatio-temporal dependences between cases and deaths The experimental results demonstrate a distinctive underlying spatio-temporal pattern between confirmed cases and deaths of the COVID-19. In Fig. 7, we report the coefficients of five representative hubs in \mathbf{A}_1 . To be specific, hubs’ coefficients in \mathbf{B}_1 , \mathbf{H}_1 , \mathbf{A}_1 indicate their spatial dependencies between each pair of past cases and current cases, past cases and current deaths, and past deaths and current deaths, respectively. As we can see, hubs have very strong “radiating” power on most of the United States regions and contribute a great deal to promote or curb the spread of the COVID-19. However, the rural area with lower population density in the Central United States is not significantly influenced by the hubs. Also, the hubs situated in the Northern United States (e.g., Chicago, New York) are negatively related to the spreading diseases to the other regions (in blue), which appear to have better controls on the expansion of the virus. In contrast, the hubs in the Southern United States (e.g., Dallas, Houston, Miami) usually are positively related to the increases of both cases and deaths in other regions (in red). In addition, the result presents some other interesting findings: some hubs show two opposite influences on the cases and deaths in the same region. For example, we see that on the one

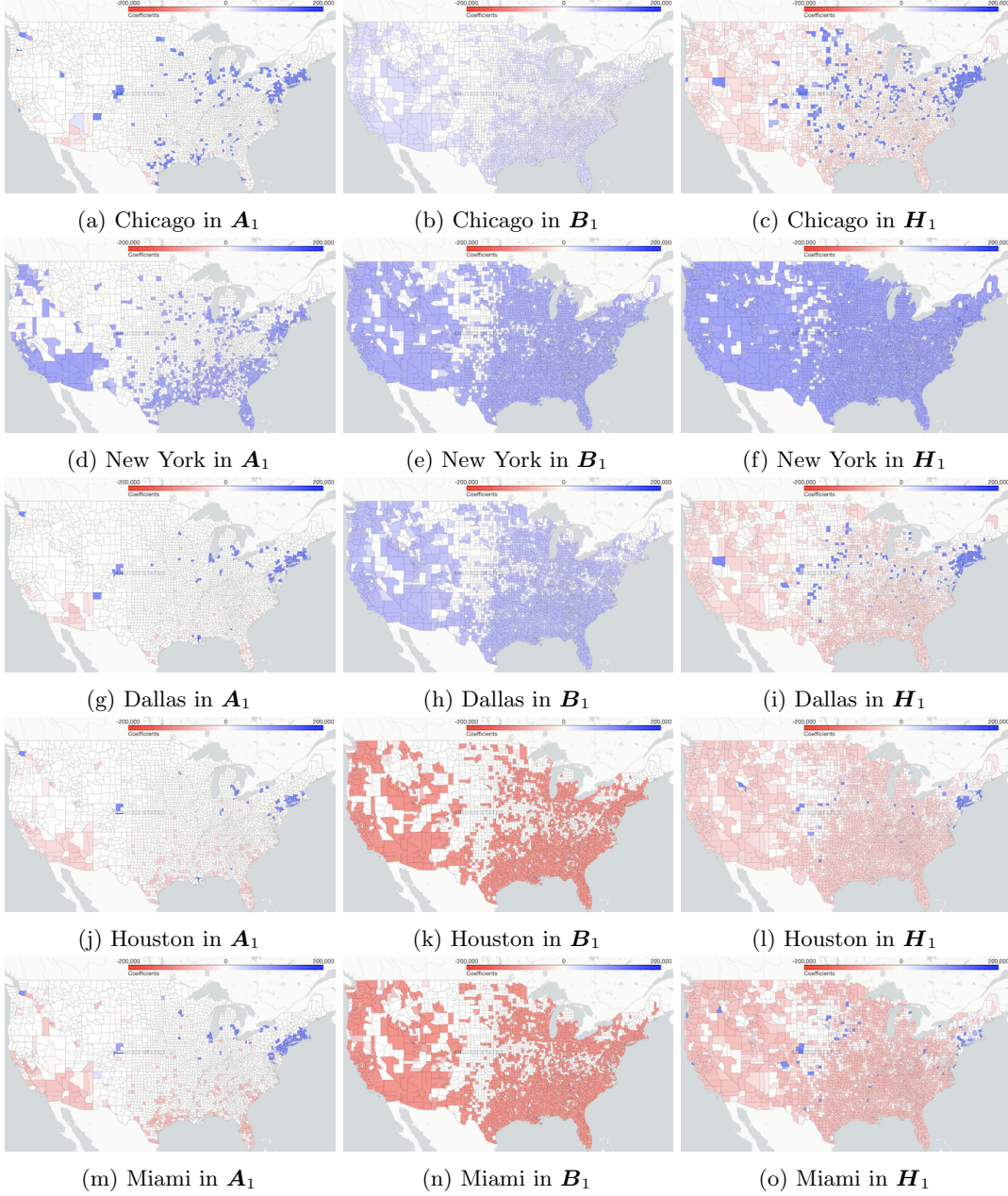


Figure 7: Examples of coefficients for hubs in matrix \mathbf{A}_1 . For instance, the color depth of any county i in (a) represents the value of coefficient $\alpha_{i,j,1}$ in \mathbf{A}_1 , where county j is Chicago. Counties in blue indicate their current number of deaths is positively related to its number of deaths in the last week; counties in red are the opposite; counties in white represent no discernable correlation between the two numbers. Coefficients of different hubs show the various spatial pattern in “spreading” or “controlling” the disease.

hand, Fig. 7 (m) shows that the number of deaths in Miami is negatively related to the deaths in the New England area of the United States. On the other hand, Fig. 7 (n) shows that the number of cases in Miami is positively related to the cases in the same area. Some hubs contribute to the increase of cases or deaths in one region, reducing the cases or deaths in other regions. For example, Fig. 7 (g) and (j) show that Dallas and Houston have a positive impact on the New England area in the United States and have a negative impact on Florida and California. In Fig. 8, we also present three typical pairs of comparisons for coefficients between one-week lag and two-week lag: coefficients of Atlanta in \mathbf{A}_1 and \mathbf{A}_2 , coefficients of Seattle in \mathbf{B}_1 and \mathbf{B}_2 , and coefficients of Los Angeles in \mathbf{H}_1 and \mathbf{H}_2 . All three comparisons share one thing in common:

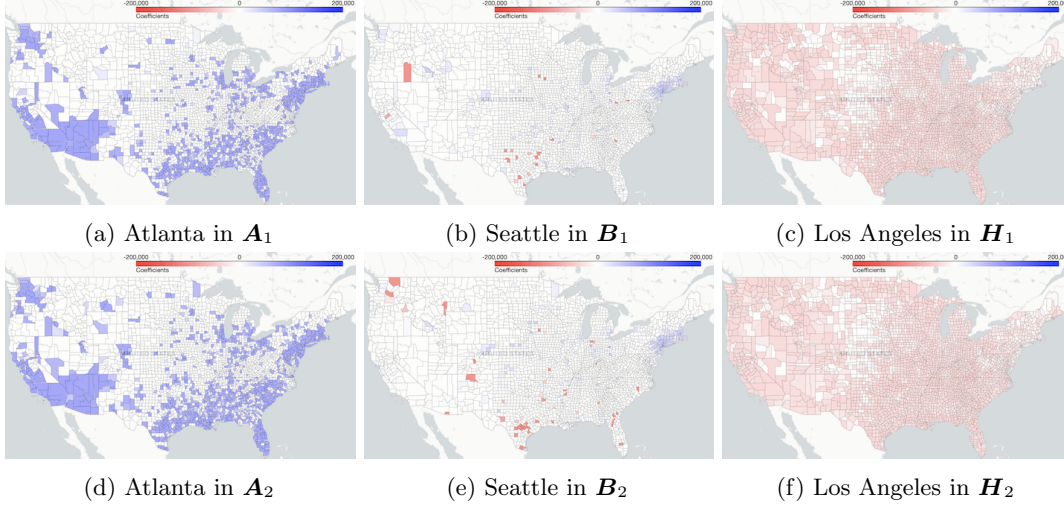


Figure 8: Examples of coefficients with different time lag.

Table 2: Summary of fitted coefficients for mobility and demographic factors. The first and second rows indicate the corresponding time lag and the category of coefficients, respectively. The first 12 columns correspond to the community mobility, and the last two columns correspond to the demographic factors. Positive coefficients have been put in bold to highlight the positive correlation with cases or deaths. The coefficients can be compared across factors as the covariates are standardized first.

Lag	One-week						Two-week						N/A	N/A
Category	Workplaces						Recreation						Population	Over 65
Term w.r.t. case	$\mu_{1,1}$	$\mu_{2,1}$	$\mu_{3,1}$	$\mu_{4,1}$	$\mu_{5,1}$	$\mu_{6,1}$	$\mu_{1,2}$	$\mu_{2,2}$	$\mu_{3,2}$	$\mu_{4,2}$	$\mu_{5,2}$	$\mu_{6,2}$	v_1	v_2
Coefficient	+9.67e+2	+1.67e+3	-1.21e+3	-7.83e+2	+3.54e+2	-5.08e+3	+1.28e+3	+2.16e+3	-8.52e+2	-7.25e+2	+3.12e+3	-5.05e+3	+2.91e+4	-1.58e+01
p-value	+5.01e-5	+3.21e-5	+1.03e-7	+7.46e-5	+2.01e-5	+2.56e-5	+2.19e-5	+2.30e-5	+3.77e-7	+3.91e-7	+1.42e-7	+6.64e-7	+9.10e-9	+1.81e-1
t-value	+5.78e+1	+7.63e+1	+1.00e+2	+1.29e+1	-7.26e+1	-5.09e+1	-4.68e+1	-4.33e+1	+2.11e+2	+1.86e+2	-3.03e+2	-3.02e+2	+1.73e+3	-9.42e-1
Term w.r.t. death	$\nu_{1,1}$	$\nu_{2,1}$	$\nu_{3,1}$	$\nu_{4,1}$	$\nu_{5,1}$	$\nu_{6,1}$	$\nu_{1,2}$	$\nu_{2,2}$	$\nu_{3,2}$	$\nu_{4,2}$	$\nu_{5,2}$	$\nu_{6,2}$	ζ_1	ζ_2
Coefficient	-1.92e+3	-1.09e+3	+3.61e+2	+1.17e+3	-3.12e+3	+4.77e+3	-1.55e+3	-9.95e+2	+2.54e+2	+1.15e+3	-3.19e+3	+4.64e+3	-1.68e+4	-1.17e+3
p-value	+2.81e-6	+4.01e-6	+1.97e-5	+7.78e-5	+4.50e-5	+9.21e-5	+1.03e-5	+3.21e-5	+8.09e-7	+3.14e-6	+9.03e-7	+9.67e-7	+1.56e-7	+6.85e-5
t-value	-1.11e+2	-9.00e+1	-6.31e+1	-5.76e+1	+2.09e+1	+1.47e+1	+6.80e+1	+6.66e+1	-1.80e+2	-1.84e+2	+2.76e+2	+2.68e+2	-9.71e+2	-6.70e+1

coefficients of different time lag have a similar spatial pattern, but the overall coefficients of two-week lag are relatively smaller than corresponding ones of one-week lag. This indicates that the last week has a stronger influence.

Dependence on local covariates Table 2 summarizes the fitted coefficients of local covariates in the model. As we can see, most of the covariates are statistically significant, with small p -values ($< .05$) except for the proportion of the elderly population age 65 and older. The positive coefficients are in bold, which indicates a positive correlation between the covariates and the cases or deaths. In particular, we observe that, for the cases, the coefficients of mobility in *workplaces*, *retail*, and *recreation*, *transit stations* have large positive values ($> 9 \times 10^2$), which indicates that the increase of mobility in these areas led to the rapid spread of the COVID-19. However, things are the opposite for the deaths, where the coefficients of mobility in *grocery* and *pharmacies*, *parks*, *residential* have large positive values ($> 2 \times 10^2$). Moreover, the population's coefficient for the cases is significantly larger than the other covariates, and it confirms that the population density is the dominant factor in spreading the disease. Last, we have found the proportion of the elderly population is significantly related to the deaths and has no clear connection to the cases.

5 Discussion

While still in the development stages, the proposed spatio-temporal model has shown immense promise in modeling and predicting the deaths and confirmed cases of COVID-19 in the United States. Nevertheless, there remains numerous open questions and rooms for improvements. For example, the uncertainty in the

count data commonly exists and can affect accuracy. It would be interesting to incorporate the serology data as an additional data source to calibrate our model. To avoid the issue of output negative output, we may adapt the current problem into a Poisson regression with log-linear model. It assumes the response variable \mathbf{x}_t has a Poisson distribution, and assumes the logarithm of its expected value can be modeled by the linear model defined in (1). In particular, this adaption plays a vital role in predicting states with fewer confirmed cases and deaths, such as Hawaii and Delaware.

References

- [1] Jérôme Adda. Economic activity and the spread of viral diseases: Evidence from high frequency data. *The Quarterly Journal of Economics*, 131(2):891–941, February 2016.
- [2] Duygu Balcan, Vittoria Colizza, Bruno Gonçalves, Hao Hu, José J Ramasco, and Alessandro Vespignani. Multiscale mobility networks and the spatial spreading of infectious diseases. *Proceedings of the National Academy of Sciences*, 106(51):21484–21489, December 2009.
- [3] The U.S. Census Bureau. American community survey, 2019.
- [4] Diego Caccavo. Chinese and italian covid-19 outbreaks can be correctly described by a modified sird model. *medRxiv*, April 2020.
- [5] Wen-Hao Chiang, Xueying Liu, and George Mohler. Hawkes process modeling of covid-19 with mobility leading indicators and spatial covariates. *medRxiv*, June 2020.
- [6] Matteo Chinazzi, Jessica T Davis, Marco Ajelli, Corrado Gioannini, Maria Litvinova, Stefano Merler, Ana Pastore y Piontti, Kunpeng Mu, Luca Rossi, Kaiyuan Sun, et al. The effect of travel restrictions on the spread of the 2019 novel coronavirus (covid-19) outbreak. *Science*, 368(6489):395–400, April 2020.
- [7] Vittoria Colizza, Alain Barrat, Marc Barthélemy, and Alessandro Vespignani. The role of the airline transportation network in the prediction and predictability of global epidemics. *Proceedings of the National Academy of Sciences*, 103(7):2015–2020, February 2006.
- [8] Chinese Center for Disease Control Epidemiology Working Group for NCIP Epidemic Response and Prevention. The epidemiological characteristics of an outbreak of 2019 novel coronavirus diseases (covid-19) in china. *Zhonghua liu xing bing xue za zhi = Zhonghua liuxingbingxue zazhi*, 41(2):145–151, February 2020.
- [9] Li-Qun Fang, Sake J De Vlas, Dan Feng, Song Liang, You-Fu Xu, Jie-Ping Zhou, Jan Hendrik Richardus, and Wu-Chun Cao. Geographical spread of sars in mainland china. *Tropical Medicine & International Health*, 14(s1):14–20, October 2009.
- [10] Jesús Fernández-Villaverde and Charles I Jones. Estimating and simulating a sird model of covid-19 for many countries, states, and cities. Working Paper 27128, National Bureau of Economic Research, May 2020.
- [11] Carlo Gaetan and Xavier Guyon. *Spatial statistics and modeling*, volume 90. Springer, New York, NY, USA, 2010.
- [12] Google. Covid-19 community mobility reports, 2020.
- [13] Tiberiu Harko, Francisco SN Lobo, and MK Mak. Exact analytical solutions of the susceptible-infected-recovered (sir) epidemic model and of the sir model with equal death and birth rates. *Applied Mathematics and Computation*, 236:184–194, June 2014.
- [14] Fiona P Havers, Carrie Reed, Travis Lim, Joel M Montgomery, John D Klena, Aron J Hall, Alicia M Fry, Deborah L Cannon, Cheng-Feng Chiang, Aridth Gibbons, et al. Seroprevalence of antibodies to sars-cov-2 in 10 sites in the united states, march 23-may 12, 2020. *JAMA Internal Medicine*, July 2020.

- [15] Herbert W Hethcote. The mathematics of infectious diseases. *SIAM review*, 42(4):599–653, October 2000.
- [16] Can Hou, Jiaxin Chen, Yaqing Zhou, Lei Hua, Jinxia Yuan, Shu He, Yi Guo, Sheng Zhang, Qiaowei Jia, Chenhui Zhao, Jing Zhang, Guangxu Xu, and Enzhi Jia. The effectiveness of quarantine of wuhan city against the corona virus disease 2019 (covid-19): A well-mixed seir model analysis. *Journal of medical virology*, 92(7):841–848, April 2020.
- [17] Jayson S Jia, Xin Lu, Yun Yuan, Ge Xu, Jianmin Jia, and Nicholas A Christakis. Population flow drives spatio-temporal distribution of covid-19 in china. *Nature*, 582(7812):389–394, April 2020.
- [18] Dayun Kang, Hyunho Choi, Jong-Hun Kim, and Jungsoon Choi. Spatial epidemic dynamics of the covid-19 outbreak in china. *International Journal of Infectious Diseases*, 94:96–102, May 2020.
- [19] Jackson A Killian, Marie Charpignon, Bryan Wilder, Andrew Perrault, Milind Tambe, and Maimuna S Majumder. Evaluating covid-19 lockdown and business-sector-specific reopening policies for three us states, May 2020.
- [20] SC Kou, Shihao Yang, Chia-Jung Chang, Teck-Hua Ho, and Lisa Graver. Unmasking the actual covid-19 case count. *Clinical Infectious Diseases*, May 2020.
- [21] Shengjie Lai, Nick W Ruktanonchai, Liangcai Zhou, Olivia Prosper, Wei Luo, Jessica R Floyd, Amy Wesolowski, Mauricio Santillana, Chi Zhang, Xiangjun Du, et al. Effect of non-pharmaceutical interventions to contain covid-19 in china. *Nature*, May 2020.
- [22] Mi Lim Lee, David Goldsman, Seong-Hee Kim, and Kwok-Leung Tsui. Spatiotemporal biosurveillance with spatial clusters: control limit approximation and impact of spatial correlation. *IIE Transactions*, 46(8):813–827, May 2014.
- [23] Lu Liu. Emerging study on the transmission of the novel coronavirus (covid-19) from urban perspective: Evidence from china. *Cities*, 103:102759, August 2020.
- [24] Fred S Lu, Andre T Nguyen, Nick Link, and Mauricio Santillana. Estimating the prevalence of covid-19 in the united states: Three complementary approaches. *medRxiv*, 2020.
- [25] Bin Meng, Jinfeng Wang, J Liu, J Wu, and E Zhong. Understanding the spatial diffusion process of severe acute respiratory syndrome in beijing. *Public Health*, 119(12):1080–1087, December 2005.
- [26] Graziano Onder, Giovanni Rezza, and Silvio Brusaferro. Case-fatality rate and characteristics of patients dying in relation to covid-19 in italy. *Jama*, 323(18):1775–1776, March 2020.
- [27] Canelle Poirier, Dianbo Liu, Leonardo Clemente, Xiyu Ding, Matteo Chinazzi, Jessica Davis, Alessandro Vespignani, and Mauricio Santillana. Real-time forecasting of the covid-19 outbreak in chinese provinces: Machine learning approach using novel digital data and estimates from mechanistic models. *Journal of medical Internet research*, 22(8):e20285, 2020.
- [28] Canelle Poirier, Wei Luo, Maimuna S Majumder, Dianbo Liu, Kenneth Mandl, Todd Mooring, and Mauricio Santillana. The role of environmental factors on transmission rates of the covid-19 outbreak: An initial assessment in two spatial scales. *Available at SSRN: <https://ssrn.com/abstract=3552677>*, March 2020.
- [29] The COVID Tracking Project. About the project, 2020.
- [30] Mohammad M Sajadi, Parham Habibzadeh, Augustin Vintzileos, Shervin Shokouhi, Fernando Miralles-Wilhelm, and Anthony Amoroso. Temperature and latitude analysis to predict potential spread and seasonality for covid-19. *Available at SSRN: <https://ssrn.com/abstract=3550308>*, March 2020.
- [31] Tanu Singhal. A review of coronavirus disease-2019 (covid-19). *The Indian Journal of Pediatrics*, 87(4):281–286, March 2020.

- [32] The New York Times. We're sharing coronavirus case data for every u.s. county, 2020.
- [33] Zifeng Yang, Zhiqi Zeng, Ke Wang, Sook-San Wong, Wenhua Liang, Mark Zanin, Peng Liu, Xudong Cao, Zhongqiang Gao, Zhitong Mai, et al. Modified seir and ai prediction of the epidemics trend of covid-19 in china under public health interventions. *Journal of Thoracic Disease*, 12(3):165–174, March 2020.